Chan-Vese Revisited: Relation to Otsu's Method and a Parameter-Free Non-PDE Solution via Morphological Framework

Arie Shaus (✉) and Eli Turkel

Department of Applied Mathematics, Tel Aviv University, Tel Aviv, Israel
ashaus@post.tau.ac.il

Abstract. Chan-Vese is an important and well-established segmentation method. However, it tends to be challenging to implement, including issues such as initialization problems and establishing the values of several free parameters. The paper presents a detailed analysis of Chan-Vese framework. It establishes a relation between the Otsu binarization method and the fidelity terms of Chan-Vese energy functional, allowing for intelligent initialization of the scheme. An alternative, fast, and parameter-free morphological segmentation technique is also suggested. Our experiments indicate the soundness of the proposed algorithm.

1 Introduction

Since its introduction at the beginning of this millennia, Chan-Vese (CV) segmentation [1] has become one of the most widely used algorithms in the field of Computer Vision. In fact, currently, with more than 8000 citations at Google Scholar, this method is almost twice as popular as the Mumford-Shah framework [2], upon which it is founded.

The power of CV technique lies within its ability to elegantly take into account the most important segmentation criteria. These include the length of the boundary curve between the segmented areas, the variance of gray-levels within each area, as well as the size of the "foreground" area. All these are handled within the scope of a single variational framework, leading to Euler-Lagrange equations, and thenceforth to numerical Gradient Descent PDE scheme. Straightforward extensions of this theme to vector-valued (e.g. RGB) images [3] (peculiarly published before [1]), as well as a multi-phase level set framework [4], were proposed by the same authors, based on the same natural formulation.

Nonetheless, CV segmentation presents its own share of challenges. Among these are several "free" parameters of the algorithm (μ , ν , λ_1 , λ_2 , ε , h , Δt ; e.g. in experimental results of [1], μ ranges from 0.0000033×255^2 to 2×255^2!), its initialization problem, as well as the intricate and sometimes computationally-intensive PDE scheme, based upon re-calculating the level set function on each step (an approach advanced by Osher and Sethian [5]). Although some of these hindrances might be handled by heuristic approaches (e.g. random re-initializations, as proposed by [1]), these are ad-hoc solutions, which add an overhead to the algorithm's implementation – with no guaranteed and sometimes difficult to forecast outcome.

Various approaches to these issues have been proposed. The method in [6] initializes using a modification of Canny edge detector [7], [8] chooses an initial level set via Gradient Descent over a thresholding criterion, [9] substitutes the level set formulation with curve evolution driven by Gaussian smoothing, [10-11] replace the energy functional with different ones working on a local level, while [12] suggests another adjustment to the functional, possessing convexity properties.

We propose a new approach: a combination of an initialization based on Otsu's binarization method [13] (proposed "heuristically" yet not justified in [14]), supplemented by a morphological non-PDE energy minimization framework. Indeed, morphological methods have been suggested in the past for minimization of energy functionals pertaining to Computer Vision in general [15-17] and CV in particular. Among the latter are: [18], replacing the energy minimization with three compound morphological operators; [19], taking into consideration some pre-computed morphological data; [20-21], utilizing various structuring elements; [22], applying morphological filters *a-posteriori*; and [23], adjusting CV energy functional by morphological gradient difference (MGD) term. The citation statistics of [13-23] suggests such methods did not win wide acceptance, possibly due to their tendency to supplement one intricate solution with another.

The main contribution of the current article is an establishment of surprising relation between CV and Otsu's method, allowing for a simple initialization procedure. We also suggest a replacement of CV's PDE with a parameter-free morphological framework. The rest of the article is organized as follows: The CV algorithm is explained, and its individual components are analyzed. An alternative algorithm is provided and tested in different settings. We conclude with summary remarks and possible future research directions.

2 The Chan-Vese algorithm

In their seminal paper [1], CV proposed the following segmentation energy functional:

$$F(c_1,c_2,C) = \mu \cdot Length(C) + \nu \cdot Area(inside(C)) + \\ +\lambda_1 \int\limits_{inside(C)} |u_0(x,y)-c_1|^2\,dxdy + \lambda_2 \int\limits_{outside(C)} |u_0(x,y)-c_2|^2\,dxdy \quad , \tag{1}$$

where $u_0(x,y)$ is a given image; c_1, c_2 are constants; $C(s)$ is a parameterized curve partitioning the image domain Ω into disjoint $inside(C)$ and $outside(C)$ sets; while μ, ν, λ_1 and λ_2 are parameters. Eq. 1 is closely related to the energy functional of Mumford and Shah [2], which can be written as:

$$F^{MS}(u,C) = \mu \cdot Length(C) + \lambda \int\limits_{\Omega} |u_0(x,y)-u(x,y)|^2\,dxdy + \alpha \int\limits_{\Omega \setminus C} |\nabla u(x,y)|^2\,dxdy \tag{2}$$

where $u(x,y)$ is the estimated image, and α is a parameter. Assuming $\alpha \to \infty$, a piece-wise-constant $u(x,y)$ is necessitated, eliminating the last term of F^{MS}. Assuming further that $u(x,y)$ has only two values, c_1 and c_2, and adding the area term, we arrive at CV functional (Eq. 1). Using the level set formulation ϕ (zero on C, positive on $inside(C)$ and negative on $outside(C)$), the Heaviside function H and Dirac's function δ_0:

$$H(z)=\begin{cases}1 & 0\le z\\ 0 & z<0\end{cases},\quad \delta_0(z)=\frac{d}{dz}H(z)\ , \tag{3}$$

Eq. 1 can be reformulated in the following fashion:

$$F(c_1,c_2,\phi)=\mu\int_\Omega \delta_0(\phi(x,y))\left|\nabla\phi(x,y)\right|dxdy+\nu\int_\Omega H(\phi(x,y))dxdy+ \tag{4}$$
$$+\lambda_1\int_\Omega \left|u_0(x,y)-c_1\right|^2 H(\phi(x,y))dxdy+\lambda_2\int_\Omega \left|u_0(x,y)-c_2\right|^2\left(1-H(\phi(x,y))\right)dxdy$$

The first variation with respect to c_1 results in:

$$c_1(\phi)=\int_\Omega u_0(x,y)H(\phi(x,y))dxdy\,/\int_\Omega H(\phi(x,y))dxdy\ , \tag{5}$$

while the first variation with respect to c_2 yields:

$$c_2(\phi)=\int_\Omega u_0(x,y)\left(1-H(\phi(x,y))\right)dxdy\,/\int_\Omega\left(1-H(\phi(x,y))\right)dxdy\ . \tag{6}$$

On the other hand, the variation with respect to ϕ is less trivial. First, [1] presents an altered version of Eq. 4, introducing regularized H_ε and δ_ε functions:

$$F_\varepsilon(c_1,c_2,\phi)=\mu\int_\Omega \delta_\varepsilon(\phi(x,y))\left|\nabla\phi(x,y)\right|dxdy+\nu\int_\Omega H_\varepsilon(\phi(x,y))dxdy+ \tag{7}$$
$$+\lambda_1\int_\Omega \left|u_0(x,y)-c_1\right|^2 H_\varepsilon(\phi(x,y))dxdy+\lambda_2\int_\Omega \left|u_0(x,y)-c_2\right|^2\left(1-H_\varepsilon(\phi(x,y))\right)dxdy$$

Next, an Euler–Lagrange equation for ϕ is derived and parameterized by an artificial time in the Gradient Descent direction:

$$\frac{\partial\phi}{\partial t}=\delta_\varepsilon(\phi)\left[\mu\cdot div\left(\frac{\nabla\phi}{|\nabla\phi|}\right)-\nu-\lambda_1\left(u_0-c_1\right)^2+\lambda_2\left(u_0-c_2\right)^2\right]\ . \tag{8}$$

A numerical scheme for Eq. 8 is also suggested, for further details see [1].

3 From Chan-Vese to Alternative Solution

We now analyze the CV algorithm, and suggest its restatement in alternative terms. In particular, we prefer not to use the level set framework. Similarly to [1], we strive to achieve a partition of the image domain Ω into two disjoint sets of pixels, denoted herein as A_1 and A_2. Unlike [1], we have no prior assumptions and no limitations regarding their location within u_0. An additional preference would be to avoid a *regularized* version of the algorithm, which tends to smooth some of the image features (cf. the criticism of CV on Gaussian smoothing in [1]).

Constants: Already in [1], it was noted that Eqs. 5 and 6 represent the averages:

$$c_1(\phi)=average(u_0)\ in\ \{0\le\phi\}\quad,\quad c_2(\phi)=average(u_0)\ in\ \{\phi<0\}\ . \tag{9}$$

Our alternative (and symmetric) formulation retains the constants c_1 and c_1, associated respectively with A_1 and A_2, and calculates them in a similar fashion:

$$c_1 = average(u_0)\ on\ A_1 \quad , \quad c_2 = average(u_0)\ on\ A_2 \ . \tag{10}$$

Localization: Eq. 8 defines the evolution of the level set, and subsequently the sets $inside(C)$ and $outside(C)$. We substitute this scheme with its morphological counterpart. We first consider the multiplicand $\delta_\varepsilon(\phi)$, where δ_ε is a regularization of δ_0. Since $\delta_0 \equiv 1$ at a zero-level $\{\phi = 0\}$, and $\delta_0 \equiv 0$ at $\{\phi \neq 0\}$, the term limits the evolution only to pixels belonging to C (optionally including their immediate neighbors for δ_ε). Agreeing with this strategy, we denote as "borderline" pixels the pixels of A_1 adjacent to at least one pixel in A_2, or vice versa.

Curvature-driven evolution: We next consider the first term of the second multiplicand of Eq. 8, $\mu \cdot div\left(\nabla\phi / |\nabla\phi|\right) - \nu - \lambda_1 (u_0 - c_1)^2 + \lambda_2 (u_0 - c_2)^2$. As explained in [4-5], $\kappa = div\left(\nabla\phi / |\nabla\phi|\right)$ is the curvature at zero level, which induces a minimization of the curve's length. This theoretical construction may be supplemented by a low-level analysis. Assuming 4-connectivity (radius of 1 around the central pixel), and taking various symmetries into account, there exists only 5 possible neighborhoods of an A_1 borderline pixel (borderline pixels of A_2 admit similar analysis). These options are presented on Fig. 1. It can be seen, that given a non-negligible μ, only Figs. 1a and 1b necessitate a re-assignment of the center pixel to A_2 - in both of these cases the radius of the osculating circle is $r = 1$, hence $\kappa = 1/r = 1$. Additionally, *ignoring the central pixel*, Figs. 1c and 1d present a symmetry between pixels assigned to A_1 and A_2, thus no re-assignment is needed (otherwise an oscillatory behavior is expected), while Fig. 1e presents a case of clear A_1 majority. The morphological operator perfectly representing such pixel assignment is the *median filter*. While the presented analysis represents a radius of 1 around the central pixel, if some kind of regularization is desired, a different median filter radius can be chosen (cf. [15,20,21] for the median filter in related contexts).

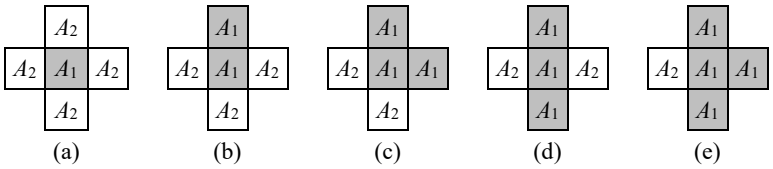

Fig. 1. Five options of neighborhood of an A_1 borderline pixel. Only (*a,b*) require a re-assignment of the central pixel, due to a positive curvature.

Area-driven evolution: The next term to be analyzed within Eq. 8 is $-\nu$. If $0 < \nu$, this represents a constant reduction in the size of $inside(C)$, which is difficult to justify (unless a human operator fancies a specific result). If for some reason the initial sets $inside(C)$ and $outside(C)$ are switched, the dynamics is reversed, as $outside(C)$ is now expected to constantly grow, breaking the symmetry between the sets. Moreover,

given images with small or zero curvature, and λ_1, λ_1 chosen to be small, the shrinking might continue until $inside(C)$ disappears completely! It seems that the dubious benefits of this term were understood by CV, since ν is mostly set to 0 in [1], and the term is no longer mentioned in [4]. We also advise against using this term, but in case it is desired, its morphological substitution would be an erosion in case of $0<\nu$, and dilation in case of $\nu<0$, with A_1 or A_2 chosen as a target.

Fidelity-driven evolution: The last terms to be considered within Eq. 8 are $-\lambda_1\left(u_0-c_1\right)^2+\lambda_2\left(u_0-c_2\right)^2$, presenting a balance between reducing the size of $inside(C)$ due to its gray-levels variance, and its enlargement due to the variance of gray-levels within $outside(C)$. Reversing our steps shows these terms originate from $\lambda_1\int_{inside(C)}\left|u_0(x,y)-c_1\right|^2 dxdy+\lambda_2\int_{outside(C)}\left|u_0(x,y)-c_2\right|^2 dxdy$ in Eq. 1, or $\lambda_1\int_{A_1}\left|u_0(x,y)-c_1\right|^2 dxdy+\lambda_2\int_{A_2}\left|u_0(x,y)-c_2\right|^2 dxdy$ in our case. Using the recommendation of $\lambda_1=\lambda_2=1$ [1], this has a surprising relation to Otsu binarization method [13] (also cf. [14]). Otsu minimizes the thresholding quality criterion $\omega_1{\sigma_1}^2+\omega_2{\sigma_2}^2$, where ${\sigma_1}^2=\sum_{i=1}^{k}\left(i-\mu_1\right)^2\cdot p_i/\omega_1$; ${\sigma_2}^2=\sum_{i=k+1}^{L}\left(i-\mu_2\right)^2\cdot p_i/\omega_2$; $\omega_1=\sum_{i=1}^{k}p_i$; $\omega_2=\sum_{i=k+1}^{L}p_i$ and p_i represents the value of the gray-level $i\in[1,2,...,L]$ within the normalized histogram of u_0. The image is thresholded by k and partitioned into disjoint sets A_1 and A_2, respectively containing gray-levels $[1,...,k]$ and $[k+1,...,L]$. Thus,

$$\omega_1{\sigma_1}^2+\omega_2{\sigma_2}^2=\int_{A_1}\left|u_0(x,y)-c_1\right|^2 dxdy+\int_{A_2}\left|u_0(x,y)-c_2\right|^2 dxdy\ . \qquad (11)$$

Eq. 11 presents us with two opportunities. Firstly, it provides an excellent option for *initialization* of the algorithm, since Otsu's method efficiently handles the needed minimization of this energy functional, with only the curve length remaining to be optimized. Secondly, it offers an explanation of the inner machinery of the fidelity term. Indeed, if all the other terms are negligible, the fidelity term would "strive" to lower the energy until the minimum, corresponding to optimal Otsu's thresholding, is reached. Therefore, several options for fidelity-driven evolution strategies can be proposed:

1. *The "original" rule*: eroding A_1 if $-\left(u_0-c_1\right)^2+\left(u_0-c_2\right)^2<0$ and dilating it if $-\left(u_0-c_1\right)^2+\left(u_0-c_2\right)^2>0$.
2. *The "Otsu-aware" rule*: At initialization, A_1 and A_2 are associated with their "optimal" partitioning (calculated only once). Even if changes in A_1 and A_2 occur due to other terms, it is still possible to immediately recognize the "misattributed" borderline pixels, which need to be re-assigned.
3. *The "no-rule" rule* (our preference): Since the initialization already used Otsu's criterion in an optimal manner, it would be better to drop the fidelity from further consideration, allowing other factors to properly influence the calculations.

Proposed algorithm: Our recommendations are summarized in Table 1.

Table 1. Description of the algorithm, including various options

Step	Recommendation	Additional options
Initialization	Otsu's method in order to partition u_0 into A_1 and A_2.	
Evolution	Median filter with radius 1* on label (A_1 and A_2) map.	Median filters with other radii* on label map, for regularization purposes.
	No area term ($\nu = 0$).	If desired, dilation/erosion of A_1 or A_2 (and vice versa).
	No fidelity term ($\lambda_1 = \lambda_2 = 0$).	• Dilation/erosion depending on fidelity term • Re-assigning "misattributed" Otsu borderline pixels
Stopping criterion	Convergence of A_1 and A_2.	

* Please note, that due to certain challenges in implementing median filters utilizing Euclidean neighborhoods, a more convenient maximum norm is used in the experimental section below. E.g., radius 1 neighborhood now includes 9 and not 5 pixels.

4 Experimental Results

In the following experiments, a segmentation is demonstrated on non-trivial images, some of which resembling the ones used by [1]. Fig. 2 presents an object with a smooth contour, Fig. 3 shows satellite image of Europe night-lights, Fig. 4 demonstrates a spiral art-work, while Fig. 5 represents a noisy inscription from the ancient biblical fort of Arad (for further details and analysis, see [24-26]). It can be observed that in general, the default or slightly regularized parameters produce high-quality segmentation, superior to Otsu with no curvature evolution. We omit comparisons with the CV algorithm, due to the high dependence of its results on the various parameters in use, as explained above.

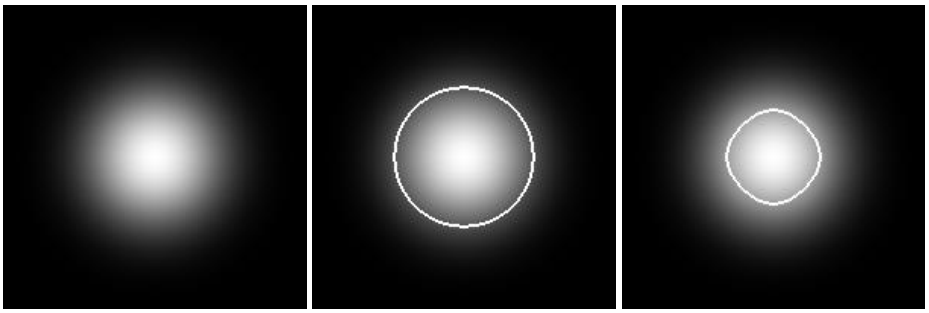

Fig. 2. Segmentation of an object of smooth contour: original image (*left*), vs. result with default setting (*center*), vs. result with radius=11 (*right*)

Fig. 3. Segmentation of a satellite image of Europe night-lights: original image (*left*), vs. Otsu binarization (*center*), vs. result with the default setting (*right*). Image courtesy NASA/Goddard Space Flight Center Scientific Visualization Studio, public domain

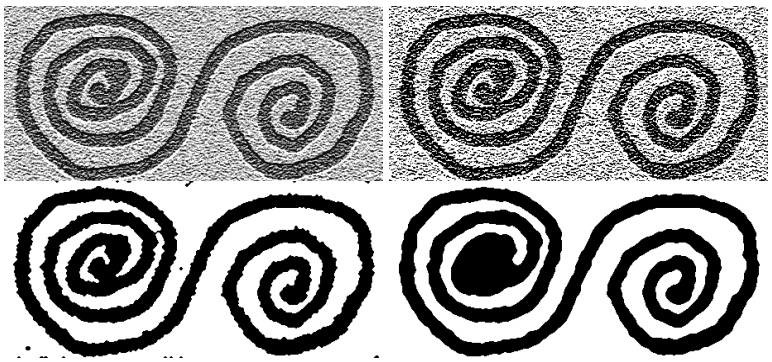

Fig. 4. Segmentation of a spiral art-work: original image (*upper left*), vs. Otsu binarization (*upper right*), vs. result with the default setting (*lower left*), vs. result with radius=2 (*lower right*). Image courtesy José-Manuel Benito Álvarez, public domain

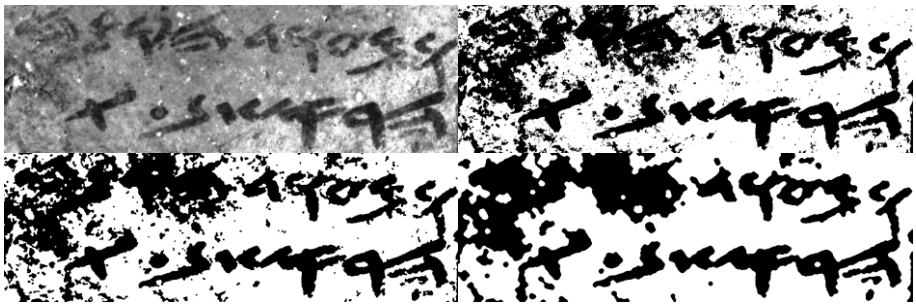

Fig. 5. Segmentation of an ancient and noisy inscription (Arad ostracon No. 1): original image (*upper left*), vs. Otsu binarization (*upper right*), vs. result with the default setting (*lower left*), vs. result with radius=2 (*lower right*). Image courtesy Institute of Archaeology, Tel Aviv University and Israel Antiquities Authority

5 Summary and Future Directions

The paper presents a detailed analysis of the CV segmentation framework. Among the main novelties of the article are the surprising relation between the Otsu binarization method and the fidelity terms of CV energy functional (which may explain the results of [12], resembling binarization), allowing for intelligent initialization of the functional. This is accompanied by a suggestion of a very fast, parameter-free morphological framework, substituting the CV PDE-based segmentation method. The experimental results demonstrate the soundness of our approach. Future research direction may include further experiments, as well as the extension of our method into vector-valued images and multi-phase segmentation.

Acknowledgements: The research received initial funding from the Israel Science Foundation – F.I.R.S.T. (Bikura) Individual Grant no. 644/08, as well as the Israel Science Foundation Grant no. 1457/13. It was also funded by the European Research Council under the European Community's Seventh Framework Programme (FP7/2007-2013)/ERC grant agreement no. 229418, and by an Early Israel grant (New Horizons project), Tel Aviv University. This study was also supported by a generous donation from Mr. Jacques Chahine, made through the French Friends of Tel Aviv University. Arie Shaus is grateful to the Azrieli Foundation for the award of an Azrieli Fellowship. The kind assistance of Dr. Shirly Ben-Dor Evian, Ms. Sivan Einhorn, Ms. Shira Faigenbaum-Golovin, and Mr. Barak Sober is greatly appreciated.

References

1. Chan, T.F., Vese, L.: Active contours without edges, IEEE Transactions on Image Processing, Vol. 10, No. 2 (2001) 266-277
2. Mumford, D., Shah, J.: Optimal approximation by piecewise smooth functions and associated variational problems, Communications on Pure and Applied Mathematics, Vol. 42 (1989) 577–685

3. Chan, T.F., Yezrielev Sandberg, B., Vese, L.: Active contours without edges for vector-valued images, Journal of Visual Communication and Image Representation, Vol. 11, Issue 2 (2000) 130-141
4. Vese, L., Chan, T.F.: A Multiphase Level Set Framework for Image Segmentation using the Mumford and Shah model, International Journal of Computer Vision Vol. 50, Issue 3 (2002) 271–293
5. Osher, S., Sethian, J.A.: Fronts propagating with curvature-dependent speed: Algorithms based on Hamilton–Jacobi Formulation, Journal of Computational Physics, Vol. 79 (1988) 12–49
6. Xia, R., Liu, W., Zhao, J., Li, L.: An optimal initialization technique for improving the segmentation performance of Chan-Vese model, Proceedings of the IEEE International Conference on Automation and Logistics (2007) 411-415
7. Canny, J.: A computational approach to edge detection, IEEE Transactions on Pattern Analysis and Machine Intelligence, Vol. 8, No. 6 (1986) 679-697
8. Solem, J.E., Overgaard, N.C., Heyden, A.: Initialization techniques for segmentation with the Chan-Vese Model, 18th International Conference on Pattern Recognition, ICPR 2006 (2006) 171-174
9. Pan, Y., Birdwell, J.D., Djouadi, S.M.: Efficient implementation of the Chan-Vese models without solving PDEs, IEEE 8th Workshop on Multimedia Signal Processing (2006) 350-354
10. Wang, X.F., Huang, D.F., Xu, H.: An efficient local Chan–Vese model for image segmentation, Pattern Recognition 43 (2010) 603-618
11. Liu, S., Peng, Y.: A local region-based Chan–Vese model for image segmentation, Pattern Recognition, Vol. 45, Issue 7 (2012) 2769–2779
12. Brown, E.S., Chan, T.F., Bresson, X., Completely convex formulation of the Chan-Vese image segmentation model, International Journal of Computer Vision, Vol. 98, Issue 1 (2012) 103–121
13. Otsu, N., A threshold selection method from gray-level histograms. IEEE Trans. Syst. Man. Cybern. Vol. 9, No. 1 (1979) 62–66
14. Xu, H., Wang, X.F.: Automated segmentation using a fast implementation of the Chan-Vese models, Proceedings of the 4th International Conference on Intelligent Computing, ICIC 2008, Advanced Intelligent Computing Theories and Applications with Aspects of Artificial Intelligence, Vol. 5227, Lecture Notes in Computer Science (2008) 1135-1141
15. Catté, F., Dibos, F., Koepfler, G.: A morphological scheme for mean curvature motion and applications to anisotropic diffusion and motion of level sets, SIAM Journal on Numerical Analysis Vol. 32, No. 6 (1995) 1895-1909
16. Álvarez, L., Baumela, L., Henríquez, P., Márquez-Neila, P.: Morphological snakes, Proceedings of the IEEE International Conference on Computer Vision and Pattern Recognition, CVPR 2010 (2010) 2197-2202
17. Welk, M., Breuß, M., Vogel, O.: Morphological amoebas are self-snakes, Journal of Mathematical Imaging and Vision Vol. 39 (2011) 87–99
18. Jalba, A.C., Roerdink, J.B.T.M., An efficient morphological active surface model for volumetric image segmentation, Proceedings of the International Symposium on Mathematical Morphology and Its Applications to Signal and Image Processing, ISMM 2009 (2009) 193-204
19. Anh, N.T.L., Kim, S.-H., Yang, H.-J.: Color image segmentation using a morphological gradient-based active contour model, International Journal of Innovative Computing, Information and Control, Vol. 9, No. 11 (2013) 4471-4484
20. Fox, V.L., Milanova, M., Al-Ali, S.: A hybrid morphological active contour for natural images, International Journal of Computer Science, Engineering and Applications, Vol. 3, No. 4 (2013) 1-13
21. Fox, V.L., Milanova, M., Al-Ali, S.: A morphological multiphase active contour for vascular segmentation, International Journal on Bioinformatics & Biosciences Vol. 3, No. 3, (2013) 1-12
22. Oliveira, R.B., Tavares, J.M.R.S., Marranghello, N., Pereira, A.S.: An approach to edge detection in images of skin lesions by Chan-Vese model, Proceedings of the 8th Doctoral Symposium in Informatics Engineering (2013)

23. Kishore, P.V.V., Prasad, C.R.: Train rolling stock segmentation with morphological differential gradient active contours, Proceedings of the International Conference on Advances in Computing, Communications and Informatics, ICACCI 2015 (2015) 1174-1178
24. Shaus, A., Turkel, E., Piasetzky, E.: Binarization of First Temple period inscriptions: Performance of existing algorithms and a new registration based scheme, 2012 International Conference on Frontiers in Handwriting Recognition, ICFHR 2012, (2012) 645-650
25. Shaus, A., Sober, B., Turkel, E., Piasetzky, E.: Improving binarization via sparse methods, Proceedings of the 16th International Graphonomics Society Conference, IGS 2013 (2013) 163-166
26. Faigenbaum-Golovin, S., Shaus, A., Sober, B., Levin, D., Na'aman, N., Sass, B., Turkel, E., Piasetzky, E., Finkelstein, I., Algorithmic handwriting analysis of Judah's military correspondence sheds light on composition of biblical texts, Proceedings of the National Academy of Sciences, Vol. 113, No. 17 (2016) 4664-4669